Journal of Alloys and Compounds 514 (2012) 91–96

Contents lists available at SciVerse ScienceDirect

Journal of Alloys and Compounds

journal homepage: www.elsevier.com/locate/jallcom

Combustion synthesis of cobalt ferrite nanoparticles—Influence of fuel to oxidizer ratio

A.B. Salunkhe, V.M. Khot, M.R. Phadatare, S.H. Pawar*

Centre for Interdisciplinary Research, D. Y. Patil University, Kasaba Bawada, Kolhapur 416006, Maharashtra, India

ARTICLE INFO

Article history:
Received 26 August 2011
Received in revised form 24 October 2011
Accepted 28 October 2011
Available online 7 November 2011

Keywords:
Nanostructured materials
Chemical synthesis
Thermodynamic properties
Scanning electron microscopy

ABSTRACT

The effect of fuel characteristics on the processing of nano-sized cobalt ferrite fine powders by the combustion technique is reported. By using different combinations of glycine fuel and metal nitrates, the adiabatic flame temperature (T_{ad}) of the process as well as product characteristics could be controlled easily. Thermodynamic modelling of the combustion reaction shows that as the fuel-to-oxidant ratio increases, the amount of gases produced and adiabatic flame temperatures also increases. The powders obtained by combustion were characterized by X-ray diffraction (XRD), scanning electron microscopy (SEM), thermo gravimetric analysis and differential thermal analysis (TG–DTA), transmission electron microscope (TEM) and vibrating sample magnetometer (VSM) measurements. The particle size of phase pure cobalt ferrite nanoparticles was found to be <40 nm in this investigation. The effects of glycine addition with stoichiometric ($\phi = 1$), fuel lean ($\phi < 1$) and fuel rich ($\phi > 1$) precursor batches were investigated separately.

1. Introduction

Spinel ferrite nanoparticles are being intensively investigated in recent years because of their remarkable electrical and magnetic properties having wide practical applications in information storage system, ferrofluid technology, magnetocaloric refrigeration and medical diagnosis [1]. Among the spinels, cobalt ferrite ($CoFe_2O_4$) is a candidate of particular interest due to its high saturation magnetization, high coercivity, strong anisotropy and excellent chemical stability. It is well known that most of the physical and chemical properties of ferrites depend strongly on the size, shape, composition and microstructure of the particles which are sensitive to the preparation methodology and preparative parameters used in their synthesis [2,3].

In recent years, synthesis of $CoFe_2O_4$ nanoparticles of desired size and magnetic properties has been the subject of investigation by many researchers. Several synthesis methods such as forced hydrolysis [4], co-precipitation [5], polyol [6], combustion reaction [7] and sonochemical [8] have been suggested for nanocrystalline $CoFe_2O_4$ preparation.

Among various methods for synthesizing ferrites, the combustion method stands out as an alternative and highly promising method [9]. Though co-precipitation is known for synthesis of fine cobalt ferrite nanoparticles, it does require careful control upon pH of the solution, concentration and temperature like parameters. On the other hand, in combustion method, it is easy to control the stoichiometry and crystallite size, which has an important influence on the magnetic properties of the ferrite. Combustion method is a low temperature synthesis technique that offers a unique mechanism via a highly exothermic redox reaction to produce oxides. The powder characteristics such as crystallite size, surface area, size distribution and nature of agglomeration are primarily governed by enthalpy or flame temperature generated during combustion which itself dependent on the nature of the fuel and fuel-to-oxidizer ratio. Among the various control parameters in a combustion process, fuel plays an important role in determining the morphology, phase, and particulate properties of the final product. Many researchers have reported combustion synthesis of $CoFe_2O_4$ nanoparticles [7,10–14]. It reveal that only glycine as a fuel was preferred to initiate the combustion reaction because of its high negative combustion heat ($-3.24\,kcal\,g^{-1}$) as compared to urea ($-2.98\,kcal\,g^{-1}$) and citric acid ($-2.76\,kcal\,g^{-1}$) [15]. Highly pure and uniform particles are essential to get the good performance of the materials with low preparation cost. With this aim, in the present work, the simple auto-combustion technique with glycine as a fuel is employed to synthesize $CoFe_2O_4$ nanoparticles, which neither requires sophisticated instrument nor the high sintering temperature.

Though nanosized $CoFe_2O_4$ were reported by combustion in literature, there is hardly any information available on the effect of reactant composition on the properties of final product. In this

* Corresponding author. Tel.: +91 231 2601202/35; fax: +91 231 2601595.
E-mail address: pawar_s_h@yahoo.com (S.H. Pawar).

0925-8388/$ – see front matter © 2011 Elsevier B.V. All rights reserved.
doi:10.1016/j.jallcom.2011.10.094

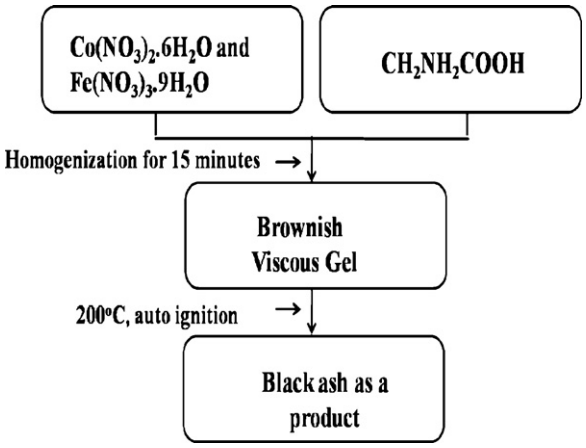

Fig. 1. Flow chart for synthesis of $CoFe_2O_4$ nanoparticles using proposed combustion method.

work, the study of reaction composition, reaction phenomena, and product characteristics are undertaken in terms of fuel to oxidizer ratio.

2. Experimental

2.1. Synthesis

The nanoparticles of cobalt ferrite were prepared by combustion method. Analytical grade cobalt nitrate [$Co(NO_3)_2{\cdot}6H_2O$] (99.8%), ferric nitrate [$Fe(NO_3)_3{\cdot}9H_2O$] (99%) were taken as oxidants while glycine [CH_2NH_2COOH] (98%) was employed as fuel to drive the combustion reaction.

According to propellant chemistry, the oxidizing and reducing valences of different elements are as follows: C = 4, H = 1, O = −2, N = 0, M = 2, 3, etc. Generally in case of ferrites, the oxidizing valence of a divalent metal nitrate $M(NO_3)_2$ becomes −10; and that for trivalent metal nitrate $M(NO_3)_3$ becomes −15, which should be balanced by total reducing valences of fuel; glycine CH_2NH_2COOH, which adds up to +9. Hence in order to release maximum energy, the stoichiometric composition of redox mixture for the reaction requires $-40 + 9m = 0$ or $m = 4.44$ mol of glycine [15,16]. Thus in order to prepare $CoFe_2O_4$, the reactants should be combined in a molar proportion of 1:2:4.44 of $Co(NO_3)_2{\cdot}6H_2O$:$Fe(NO_3)_3{\cdot}9H_2O$:CH_2NH_2COOH, respectively. Under equilibrium condition, combustion reaction can be expressed as follows:

$$Co(NO_3)_2{\cdot}6H_2O + 2Fe(NO_3)_3{\cdot}9H_2O + 4.44\phi NH_2CH_2COOH$$
$$+(9.99\phi - 10)O_2(g) \rightarrow CoFe_2O_4 + 8.88\phi CO_2(g) + (24 + 11.1\phi)H_2O(g)$$
$$+(4 + 2.22\phi)N_2(g)(28 + 22.2\phi)\text{moles of gas} \quad (1)$$

where ϕ is the multiplication factor in order to get fuel lean ($\phi < 1$), fuel stoichiometric ($\phi = 1$), and fuel rich condition ($\phi > 1$). In above reaction $\phi = 1$ represents G/N = 4.44/3 = 1.48 and it is the stoichiometric condition for present case (i.e. the ratio at which oxygen content of oxidizer can be reacted to consume fuel entirely and no heat exchange is required for the complete reaction).

In typical procedure, the stoichiometric amounts (G/N = 1.48) of cobalt nitrate, ferric nitrate and glycine were taken in a glass beaker. The precursors resulted in slurry after mixing for 15 min due to hygroscopic nature of the metal nitrates. The beaker was then kept on hot plate preheated to 200 °C. The whole combustion reaction process was complete in less than 15 min whereas actual time of ignition was less than 5 s. During combustion, a great deal of foams produced and spark appeared at one corner which spread out through the mass, yielding a voluminous and fluffy product in the beaker. The general flow chart of the synthesis process is shown in Fig. 1. In the present paper, glycine to nitrate (G/N) molar ratio has been varied as 0.74, 1.48 and 2.22 to obtain fuel lean, stoichiometry and fuel rich conditions, respectively. This synthesis route was without any subsequent heat step.

2.2. Characterization

Thermo gravimetric analysis and differential thermal analysis of stoichiometric precursors have been carried out with the help of transanalytical instrument (SDT 2960) operated in temperature range 35–1000 °C with heating rate of 10 °C per minute in flowing air ambience. Crystallite phase identification and crystalline size determination of combusted nanoparticles were carried out by using Philips PW-3710 automated X-ray diffractometer equipped with a crystal monochromator employing Cr-Kα radiation of wavelength 2.28970 Å. The crystallite size (D) was calculated from X-ray line broadening of the (3 1 1) diffractions peak using Debye Scherrer formula

$$D = \frac{0.9\lambda}{\beta \cos\theta} \quad (2)$$

where β is the full-width at half maxima of the strongest intensity diffraction peak (3 1 1), λ is the wavelength of the radiation and θ is the angle of the strongest characteristic peak. Surface morphology of the synthesized nanoparticles was observed with JEOL JSM 6360 SEM with magnification of about 15,000×. The particle size of the $CoFe_2O_4$ nanoparticles was measured with TEM (Philips CM 200 model, operating voltage 20–200 kV, resolution 2.4 Å). The magnetic characterizations were done by VSM (Lake Shore 7307 model) under the applied field of ±9000 Oe at room temperature.

3. Results and discussion

3.1. TG–DT analysis

The simultaneous TG–DTA curves of the stoichiometric metal nitrates without glycine (fuel) and stoichiometric metal nitrates with glycine were shown in Fig. 2A and C, respectively. From Fig. 2A, it is observed that metal nitrates (i.e. $Co(NO_3)_2{\cdot}6H_2O$ and $Fe(NO_3)_3{\cdot}9H_2O$) can be completely decomposed into their respective oxides above 250 °C with weight loss of ∼75%. The TG–DTA curve for pure glycine is shown in Fig. 2B. The DTA curve of pure glycine contains sharp endothermic peak at about 280 °C with weight loss of about 63% and three exothermic peaks in temperature range of 300–600 °C accompanied with 37% weight loss corresponding to complete decomposition of carbonaceous matter.

In TG–DTA curve of metal nitrates with glycine (Fig. 2C) it is observed that, there is presence of small endothermic peak at 130 °C accompanied with ∼2% weight loss which was attributed to vaporization of inner water. The exothermic peak with sharp weight loss observed around 176 °C (Fig. 2C) indicates occurrence of combustion reaction during the decomposition of the nitrate–glycine dried gel. The requirement of lower temperature for the combustion reaction using glycine as a fuel may be due to higher value of heat of combustion of glycine [17]. The observed weight loss associated with the exothermic reaction is approximately 56%. No weight loss is observed after the combustion reaction giving a product free of residual reactants and carbonaceous matter. The total weight losses observed in TGA plot of precursors is ∼74% whereas the expected weight loss corresponding to the complete conversion of precursors to $CoFe_2O_4$ is ∼83% which is in good agreement with the value calculated from Eq. (1) [14]. By accompanying the TG–DTA curves of the metal precursors with and without fuel, it can be suggested that acceleration of the reaction rate (i.e. slope of weight loss curve is very steep) and lowering of the decomposition temperature may be attributed to the presence of nitrate ions in the precursor since NO_3^- ions provide an in situ oxidizing environment for the oxidation of the organic reaction temperature and increase in reaction rate results in a combustion reaction of the glycine–nitrate precursor.

3.2. Combustion mechanism and thermodynamic consideration

There would be different mechanism of combustion reaction with different fuel-oxidizer combinations. When a mixture containing oxidizer and fuel with required stoichiometry is heated rapidly at or above the temperature of exothermic decomposition of fuel, it undergoes melting and dehydration initially. Later on this mixture foams due to the generation of gaseous decomposition products as intermediates and leads to enormous swelling. The gaseous decomposition products would be a mixture of nitrogen oxides, NH_3, and HNCO. These gases are known to be hypergolic in contact with each other. The foam could be made up of polymers like cyanuric acid, polymeric nitrate, etc. which are combustible. Consequently, the foam breaks out with a flame because of the

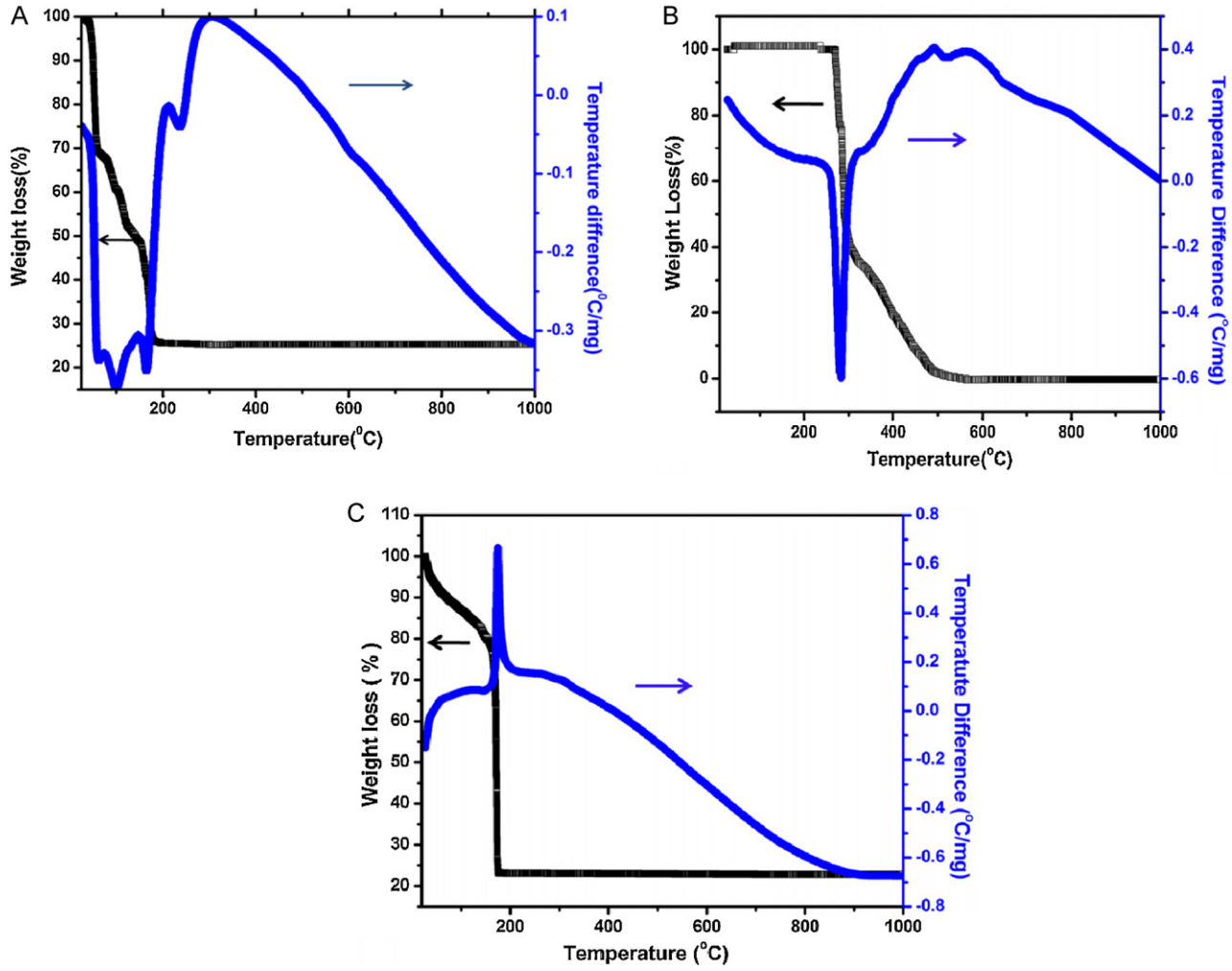

Fig. 2. TG–DTA curves of the (A) precursors (mixture of metal nitrates without glycine), (B) glycine and (C) precursors gel (mixture of metal nitrates with glycine).

accumulation of the hypergolic mixture of gases. With an in situ temperature build-up of >1000 °C the whole foam further swells and burns with flames. At such a high in situ temperature, the foam decomposes to maximum yield product. However, in cases where the gases responsible for combustion are allowed to escape or when their densities are less or the required temperature is not met, the combustion does not occur with a flame. The foam only sustains combustion but itself does not initiate ignition. In addition, if the mixture is heated at a slow rate the flame does not appear, since the time required to reach the ignition temperature is longer and all the gases responsible for combustion escape the foam [18].

In order to study relative exothermicity of combustion reaction involving different G/N ratio, a simplified thermodynamic approach has been taken. The calculations based on thermodynamic considerations have been carried out to predict the exact situations and ignition of reaction. Adiabatic flame temperature T_{ad} is used to define the temperature at which the enthalpies of the products are equal to those of reactants. If all heat generated heats up the product and no heat exchange take place with the surroundings, then T_{ad} can be calculated using the following equations:

$$Q = -\Delta H^\circ = \int_{298}^{T_{ad}} \left(\sum n.C_p\right)_{\text{products}} dT \quad (3)$$

where Q is the heat absorbed by products under adiabatic condition, and C_p is the heat capacity of the products at constant pressure. For adiabatic calculations, room temperature is considered as reference, $T_o = 298$ K. The change in enthalpy of reaction (ΔH°) can be expressed as:

$$\Delta H^\circ = \sum n(\Delta H^\circ_f)_{\text{products}} - \sum n(\Delta H^\circ_f)_{\text{reactants}} \quad (4)$$

where, n is the number of moles and ΔH°_f is the enthalpy of formation. Thermodynamic data of various reactants and products is well available in literature [6,19,20]. For the present case it is listed in Table 1. Substituting corresponding values from Table 1 in Eq. (3), the enthalpy of reaction as a function of the ϕ can be obtained as follows:

$$\Delta H^\circ = 459.93 + \phi(-1122.71) \quad (5)$$

Using the thermodynamic data from Table 1, Eqs. (3) and (5), adiabatic flame temperature (T_{ad}) for various ϕ values can be

Table 1
Thermodynamic data required for calculating adiabatic flame temperature.

Compound	H°_f (kcal mol^{-1})	C_p (cal mol^{-1} K^{-1})
$Co(NO_3)_2{\cdot}6H_2O$	−528.49	–
$Fe(NO_3)_2{\cdot}9H_2O$	−785.2	–
H_2O(g)	−57.79	$7.2 + 0.0036T$
O_2 (g)	0	$5.92 + 0.00367T$
$CoFe_2O_4$	−252.0	$10.34 + 0.00274T$
CO_2 (g)	−94.05	35.36
N_2 (g)	0	$6.5 + 0.00100T$

Where, T is the absolute temperature.

Table 2
Effect of fuel-to-oxidizer ratio on moles of gases evolve, heat of formation of product and adiabatic temperature.

Multiplication factor 'ϕ'	G/N ratio	Heat of formation of product $\Delta H^{\circ}_{combustion}$ Kcal/mol	Adiabatic flame temperature T_{ad} in K	Amount of gases produced during combustion (moles)
0.5	0.74 (fuel lean)	−101.425	576.5	39.1
1	1.48 (stoichiometry)	−662.780	1717.1	50.2
1.5	2.22 (fuel rich)	−1224.135	2445.6	61.3

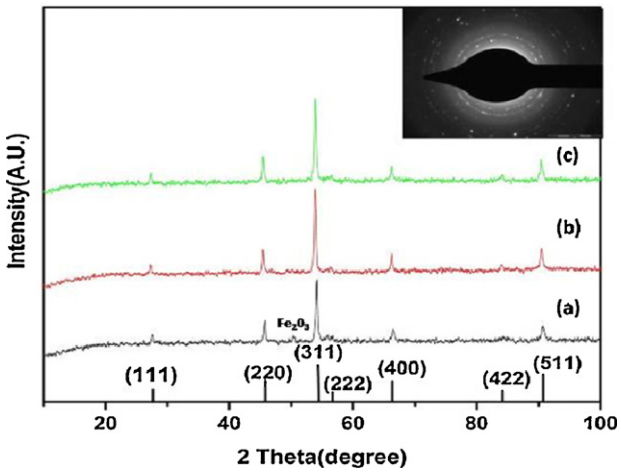

Fig. 3. Typical X-ray diffraction pattern of $CoFe_2O_4$ with different G/N ratio (a) for G/N = 0.74, (b) for G/N = 1.48 and (c) for G/N = 2.22.

calculated. The variation of enthalpy and adiabatic flame temperature with the glycine-to-nitrate molar ratio were presented in Table 2. As expected, these values increase substantially with the amount of fuel used during combustion. The values indicate that the heat of combustion is significant for all conditions such as fuel lean, stoichiometry and fuel rich.

The amount of fuel is minimum in case of fuel lean system that result in small value of enthalpy as compared to the fuel rich and fuel stoichiometric systems. In fuel lean case there is more oxidants than reductants, i.e. it sets the system as an over-oxidizing state where, the excess oxygen must be heated to the product temperature. Thus the product temperature decreases from stoichiometric value indicating the systems departure from equilibrium state [21,22]. Therefore local temperature of the particles in fuel lean case is minimum and it may prevent the formation of dense structure. However, the associated evolution of gases during the combustion reaction results in highly porous structure. Table 2 shows that, as G/N molar ratio increases the adiabatic flame temperature and enthalpy of reaction increases with an increment in the total number of mole of gases evolved during the reaction. Our results tend to indicate that glycine to nitrate molar ratio plays a predominant role for stoichiometric, fuel-lean and fuel-rich compositions.

3.3. Structural analysis

The structural properties of $CoFe_2O_4$ samples prepared with fuel lean, stoichiometric, fuel rich conditions were studied by X-ray diffractometer and the patterns were shown in Fig. 3. In addition, the selected area electron diffraction (SAED) pattern shown in the upper right inset of Fig. 3 can be well indexed to (1 1 1), (2 2 0), (3 1 1), (4 0 0), (4 2 2), (5 1 1) and (4 4 0) of cubic spinel structure, which is consistent with the result of XRD. The obtained peaks are well matched with standard JCPDS card no. 22-1086. From the Debye Scherer formula, it was found that all the samples obtained are nanocrystalline with the sizes ranging between 30 and 40 nm. Weak diffraction peak corresponding to formation of Fe_2O_3 was observed in case of sample prepared by fuel lean condition (Fig. 3a). This was due to the fact that inadequate fuel could not react completely with metal nitrates to release enough heat to form well developed phase of $CoFe_2O_4$.

XRD data enables us to investigate the role of G/N ratio in modifying the structural parameters such as crystallite size (D), lattice constant (a), X-ray density (D_x), unit cell volume (V) for combusted cobalt ferrite. The estimated values of various structural parameters are given in Table 3. It can be seen from table that the value of D and V increases linearly with increase in G/N ratio. On the other hand X-ray density is found to decreases with increase in amount of glycine. However, there is no remarkable difference in value of lattice constant thereby indicating efficiency of combustion method for preparation of $CoFe_2O_4$ [13]. The observed increase in crystallite size could be attributed to an increase in flame temperature which assists crystal growth [10]. The observed decrease in density of resulting product due to increase in glycine content could be attributed to reduction of oxygen vacancies which play a predominant role in accelerating densification, i.e. the decrease in oxygen ion diffusion would retard the densification [23].

3.4. Morphological analysis

The morphology of the prepared samples was determined by SEM and is shown in Fig. 4. These images revealed remarkable changes in microstructure, regarding grain size, porosity, and particle distribution by changing G/N ratio. However, the voids and pores present in the samples are attributed to the release of large amount of gases during the combustion process. For G/N = 0.74 (Fig. 4a), agglomerated oval shape morphology is observed, while few semi-spherulitic are also visible. It is clear from Fig. 4b that at stoichiometric ratio G/N = 1.48, the oval shape vanishes and crystallites scatter in all direction may be due to evolution of large amount of heat and initiation of flame. For further increase in G/N = 2.22, typical porous foam like network is formed probably due to escaping gases during combustion reaction (Fig. 4c) [20]. It can be concluded that the morphology of the $CoFe_2O_4$ nanoparticles depends highly on amount of glycine added to initiate the combustion process. When the flame temperature increased using calculated amount of glycine, a radical change in the microstructure was observed.

Table 3
The effect of G/N ratio on structural properties of $CoFe_2O_4$ nanoparticles.

G/N ratio	Crystallite size 'D' in nm	Lattice constant 'a' in nm	Unit cell volume 'V' in nm^{-3}	X-ray density 'D_x' in g/cm^3
0.74 (fuel lean)	33	0.8364	0.5851	5.1459
1.48 (stoichiometry)	37	0.8376	0.5876	5.1231
2.22 (fuel rich)	38	0.8377	0.5878	5.1213

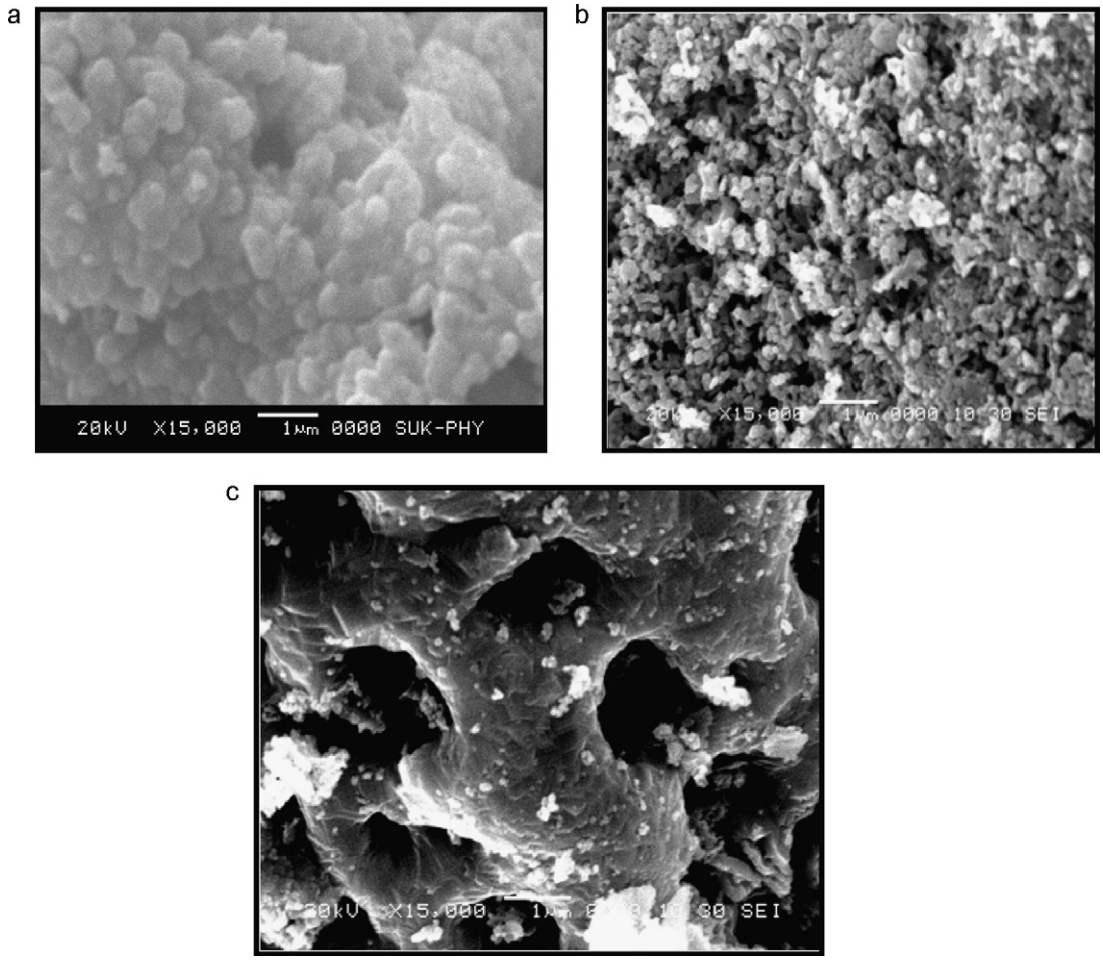

Fig. 4. SEM images of $CoFe_2O_4$ with different G/N ratio (a) for G/N = 0.74, (b) for G/N = 1.48 and (c) for G/N = 2.22.

The TEM images of the combusted product (G/N = 1.48 and 2.22) were shown in Fig. 5a and b. It shows the typical nearly spherical nanocrystalline $CoFe_2O_4$ with which to confirm lower particle size distribution in case of fuel rich ratio in comparison with stoichiometric ratio. Furthermore the average particle sizes measured by TEM for $CoFe_2O_4$ particles prepared through stoichiometric and fuel rich systems are ~34 and 37 nm which is in good agreement with the particle sizes calculated by XRD analysis.

3.5. Magnetic properties

The $CoFe_2O_4$ with an inverse spinel structure shows ferromagnetism that originates from magnetic moment of antiparallel spins between Fe^{3+} ions at octahedral sites and Co^{2+} ions at tetrahedral sites [18]. The dependence of the magnetization and magnetic moment on the grain size is explained on the basis of changes in exchange interaction between tetrahedral and octahedral lattices.

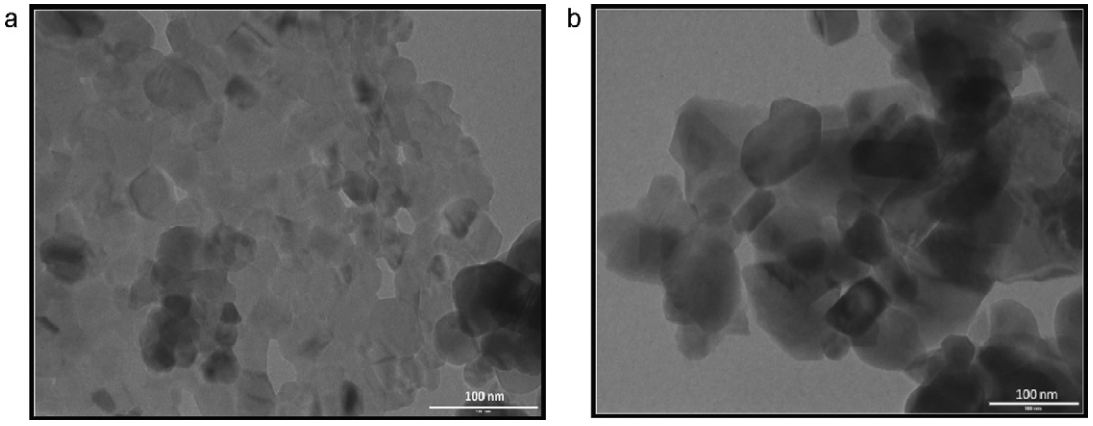

Fig. 5. TEM images of $CoFe_2O_4$ powder obtained through: (a) the stoichiometric and (b) the fuel rich samples.

Table 4
The effect of G/N ratio on magnetic properties of $CoFe_2O_4$ nanoparticles.

G/N ratio	Saturation magnetization 'M_s' in emu/g	Remanence magnetization 'M_r' in emu/g	Coercivity in 'Oe'	M_r/M_s
0.74 (fuel lean)	33	17.07	1168	0.502
1.48 (stoichiometry)	45	22.91	1051.3	0.509
2.22 (fuel rich)	59	28.09	820.4	0.47

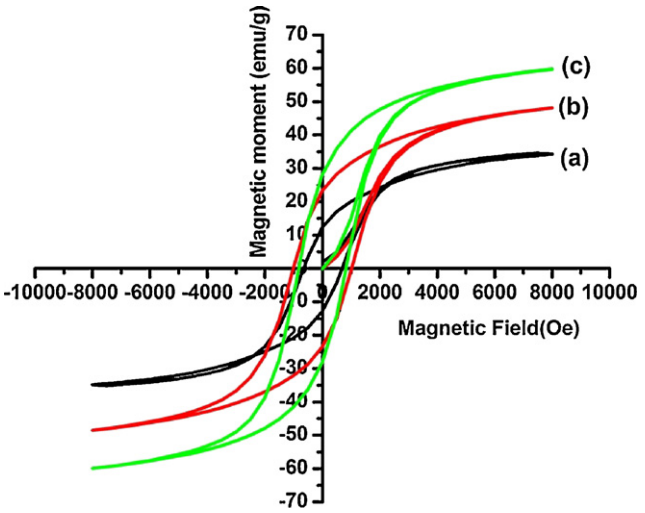

Fig. 6. Magnetic hysteresis curves measured at room temperature for (a) the stoichiometric and (b) the fuel rich samples.

The hysteresis loops measured at room temperature for as synthesized samples are shown in Fig. 6. These curves are typical for hard magnetic materials with high saturation magnetization and remanence. The saturation magnetization increases from 33 to 59 emu/g and remanence magnetization increases from 17 to 28 emu/g systematically with increase in amount of glycine in combustion reaction. The saturation magnetization (M_s), remanence magnetization (M_r), coercivity (H_c) and loop squareness ratio M_r/M_s were summarized in Table 4. Clearly the magnetic properties of $CoFe_2O_4$ nanoparticles show dependence upon adopted adiabatic flame temperature during combustion reaction. From Table 4, one can conclude that, the evolution behaviour of M_r and M_s are highly depending upon the growth of $CoFe_2O_4$ nanoparticles. Both M_s and M_r increases with the increase in amount of fuel used in combustion. Crystallinity of samples is also found to increase with increase in amount of glycine used for the combustion. The increase in crystallinity with higher glycine amount results in burst increase in magnetization values. However, difference in crystallization process could influence the distribution of Co^{2+} ions at octahedral Fe^{3+} between tetrahedral and octahedral sites, and then further affect the super-exchange interaction between two ions. The low magnetization value (33 emu/g) is observed for fuel lean condition. This could be the consequence of the wide particle size distribution, where there is a small fraction of super-paramagnetic particles contributing to reducing magnetization. The presence of canted anti-ferromagnetic α-Fe_2O_3, may contribute to the reduction in magnetization.

4. Conclusion

A simple wet chemical process based on glycine–nitrate combustion has been studied to demonstrate the effect of G/N molar ratio on the phase stability, microstructure and size of $CoFe_2O_4$ nanoparticles. The size of the nanoparticles increases linearly with flame temperature due to coalescence of these particles depending upon the released heat during combustion process. A thermodynamic consideration of the combustion reaction shows that when G/N molar ratio increases, the amount of gas produced and adiabatic flame temperature also increases. The much pronounced effect was observed in case of morphology of the products. The grain size was found to be increased with an increase in G/N molar ratio. Increases in number of moles of gases escaped during the combustion with increasing G/N molar ratios may be responsible for the formation of fluffy or porous structure of the material. All of the $CoFe_2O_4$ nanoparticles, having their hysteresis loop in the range of $-9000 < H_c < 9000$ Oe, with the specific magnetizations 33, 45 and 59 emu/g of for the fuel lean, fuel sufficient and fuel rich samples, respectively.

Acknowledgements

Authors are grateful to BRNS, DRDO and DST for their financial support for this research work.

Appendix A. Supplementary data

Supplementary data associated with this article can be found, in the online version, at doi:10.1016/j.jallcom.2011.10.094.

References

[1] L. Zhao, H. Yang, L. Yu, Y. Cui, X. Zhao, B. Zou, S. Feng, J. Magn. Magn. Mater. 301 (2006) 445–451.
[2] E.K. Mooney, J.A. Nelson, M.J. Wagner, Chem. Mater. 16 (2004) 3155–3161.
[3] D.R. Cornejo, A. Medina-Boudri, H.R. Bertorello, J. Matutes-Aquino, J. Magn. Magn. Mater. 242 (2002) 194–196.
[4] G.V. Duong, N. Hanh, D.V. Linh, R. Groessinger, P. Weinberger, E. Schafler, M. Zehetbauer, J. Magn. Magn. Mater. 311 (2007) 46–50.
[5] N. Millot, S.L. Gallet, D. Aymes, F. Bernard, Y. Grin, J. Eur. Ceram. Soc. 27 (2007) 921–926.
[6] G. Baldi, D. Bonacchi, C. Innocenti, G. Lorenzi, C. Sangregorio, J. Magn. Magn. Mater. 311 (2007) 10–16.
[7] A.F. Júnior, E.C. De Oliveira Lima, M.A. Novak, P.R. Wells Jr., J. Magn. Magn. Mater. 308 (2007) 198–202.
[8] S.I. Park, J.H. Kim, C.G. Kim, C.O. Kim, Curr. Appl. Phys. 8 (2008) 784–786.
[9] A.C.M. Costa, E. Tortella, M.R. Morelli, M. Kaufman, R.H.G.A. Kiminami, J. Mater. Sci. 37 (2002) 3569–3572.
[10] N.M. Deraz, J. Anal. Appl. Pyrolysis 88 (2010) 103–109.
[11] L. Ai, J. Jiang, Curr. Appl. Phys. 10 (2010) 284–288.
[12] R.S. de Biasi, A.B.S. Figueiredo, A.A.R. Fernandes, C. Laricab, Solid State Commun. 144 (2007) 15–17.
[13] C-H. Yan, Z.G. Xu, F.X. Cheng, Z.M. Wang, L.D. Sun, C.S. Liao, J.T. Jia, Solid State Commun. 111 (1999) 287–291.
[14] S.H. Xiao, W.F. Jiang, L.Y. Li, X.J. Li, Mater. Chem. Phys. 106 (2007) 82–87.
[15] A.F. Junior, T.E.P. Alves, E.C. de, O. Lima, E. da, S. Nunes, V. Zapf., Appl. Phys. A 94 (2009) 131–137.
[16] S.R. Jain, K.C. Adiga, Combust. Flame 40 (1981) 71–79.
[17] R.K. Lenka, T. Mahata, P.K. Sinha, A.K. Tyagi, J. Alloys Compd. 466 (2008) 326–329.
[18] K.C. Patil, M.S. Hegde, T. Rattan, S.T. Aruna, Chemistry of Nanocrystalline Oxide Materials, World Scientific Publishing Co. Pte. Ltd., USA, 2008.
[19] J.A. Dean, Lange's Handbook of Chemistry, fifteenth ed., McGraw-Hill, New York, 1998.
[20] J. Leitner, P. chuchvalee, D. Sedmidubsky, A. Streje, P. Abrman, Thermochim. Acta 93 (2003) 27–46.
[21] J.C. Toniolo, M.D. Lima, A.S. Takimi, C.P. Bergmann, Mater. Res. Bull. 40 (2005) 561–571.
[22] S.K. Sharma, S.S. Pitale, M. Malik, R.N. Dubey, M.S. Qureshi, S. Ojha, Physica B 405 (2010) 866–874.
[23] A. Alarifi, N.M. Deraz, S. Shaban, J. Alloys Compd. 486 (2009) 501–506.